Fixed-order Linear Parameter Varying Controller Design for a 2DOF Gyroscope ⋆

Zlatko Emedi * **Alireza Karimi** *

* *Laboratoire d'Automatique*
Ecole Polytechnique Fédérale de Lausanne, Switzerland

Abstract: This paper presents an approach for fixed-order Linear Parameter Varying (LPV) controller design with application to a 2 Degree-of-Freedom (2DOF) gyroscope experimental setup. Inner convex approximation of the non-convex set of all stabilizing fixed-order LPV controllers is characterized through a set of Linear Matrix Inequalities (LMIs). This is achieved through the use of two slack matrices which enable decoupling of the controller and Lyapunov matrix parameters in the derivative of Lyapunov function. The LPV model obtained by the approximation of the nonlinear model of the 2DOF gyroscope is used for the design of a second-order LPV controller. Experimental results show good tracking performance in the presence of scheduling parameter variations.

Keywords: LPV System Control; Fixed-order Controller Design; LMIs in Control; Parameter Dependent Lyapunov Function; 2DOF Gyroscope.

1. INTRODUCTION

In the previous two decades, the modeling and control of LPV systems has become a very important area of research (Leith and Leithead (2000); Shamma (2012)). The motivation for this development is the use of linear systems theory tools on a wide class of nonlinear systems (Shamma and Athans (1991)). Over the years, the theory of LPV systems has been successfully applied to modeling and control in different practical applications, e.g. for wind turbine control (F. D. Bianchi et al. (2004); F. D. Adegas et al. (2012)), turbofan engines (W. Gilbert et al. (2010); Balas (2002)), wafer stage (Wassink et al. (2005)), missile autopilot design (J-M Biannic and P. Apkarian (1999); P. C. Pellanda et al. (2002); L. H. Crater and J. S. Shamma (1996); F. Wu et al. (1995)) and active braking control (G. Panzani et al. (2012)).

LPV systems are characterized by linear-like models depending on time-varying measured signals, which we usually refer to as scheduling parameters. An important aspect of any LPV control approach is the way the scheduling parameters are handled in the design process. In some of the approaches (e.g. Apkarian and Gahinet (1995)) Linear Fractional Transformation (LFT) framework is used to isolate the scheduling parameters. This allows the small-gain theorem to be used for the analysis of system's stability, but it can introduce some conservatism for the way scheduling parameters are structured and for the use of single Lyapunov function for ensuring the closed-loop stability. However, the system will remain stable even for infinitely fast variations of scheduling parameters. It should be mentioned that some systems are not stabilisable using a single quadratic Lyapunov function (F. Wu et al. (1996)), and often the bounds on the variation rate are known. Therefore, considering a bound on the variation rate of scheduling parameters certainly relaxes the controller synthesis problem.

Parameter Dependent Lyapunov Functions (PDLF) are used for the uncertain and LPV system analysis and synthesis in e.g. J. C. Geromel et al. (1998); Geromel et al. (2007); F. Wu et al. (1996); Apkarian and Adams (1998). In F. Wu et al. (1996) both state-feedback and full-order output feedback LPV controller design are treated, while only the output-feedback controller design is considered in Apkarian and Adams (1998). Both these approaches lead to controller matrices that depend on the derivative of the scheduling parameter, which is not measurable in the general case. In the latter, this can be avoided by fixing a part of the structured Lyapunov matrix and the use of a scaling matrix for reducing the conservatism of the approach. The approach developed in Sato (2011) represents the extension of the output-feedback LPV controller design method from Apkarian and Adams (1998). It gives at worst the same performance as the one in Apkarian and Adams (1998), but at a cost of increased computation time.

Practical implementation of LPV controllers is in general a complex task. In the state-feedback case, it is necessary to measure or estimate all the states of an LPV system. Full-order output-feedback LPV controllers can be of high order, equal to the order of an augmented plant. For both approaches, usually some tedious linear algebra has to be applied online, including matrix inversion, which limits the use of such controllers. For these reasons, there exists a need for fixed-order output-feedback LPV controller synthesis methods. Some methods for fixed-order LPV controller design with a scheduling parameter dependent transfer function representation are presented in W. Gilbert et al. (2010); S. Formentin et al. (2013); Z. Emedi and A. Karimi (2012). These methods are based on

⋆ This research work is financially supported by the Swiss National Science Foundation under Grant No. 200021-121749.

extension of robust controller design methods for polytopic uncertain systems (Henrion et al. (2003); H. Khatibi and A. Karimi (2010)) to LPV systems. One drawback of these methods is that the transfer function representation of LPV system often depends in a polynomial fashion on scheduling parameters. The other adverse side is the extension of the approach to MIMO systems which could be very involved as all transfer functions would have to be brought to the common denominator, increasing the complexity of the plant models.

A method for fixed-order output-feedback LPV controller design for state-space LPV plant models with affine dependence on the scheduling parameter vector is presented in Z. Emedi and A. Karimi (2013). The method is extended in this paper through an addition of a slack matrix parameter and extended method is applied to a 2DOF gyroscope experimental setup. In Section 2 some preliminaries are provided. Section 3 presents the main aspects of the method. Section 4 describes the LPV modeling of the gyroscope experimental setup, controller design and implementation details and the experimental results. Finally, the content of the paper is summarized in Section 5.

2. PRELIMINARIES

Considered LPV plant model and controller structure are presented. Next, the stability conditions for the closed-loop LPV system are discussed.

2.1 Plant model structure

Considered plant model is assumed to belong to the class of continuous-time LPV systems:

$$\begin{aligned}\dot{\mathbf{x}}_g(t) &= A_g(\boldsymbol{\theta}(t))\mathbf{x}_g(t) + B_g(\boldsymbol{\theta}(t))\mathbf{u}(t) \\ \mathbf{y}(t) &= C_g\mathbf{x}_g(t),\end{aligned} \tag{1}$$

where vector $\mathbf{x}_g(t)$ represents the state vector in $\mathbb{R}^n$, $\mathbf{u}(t)$ is the control input vector in $\mathbb{R}^{n_u}$, and $\mathbf{y}(t)$ is the plant output vector in $\mathbb{R}^{n_y}$. Scheduling parameter vector $\boldsymbol{\theta}(t) = [\theta_1(t), \ldots, \theta_{n_\theta}(t)]'$ belongs to a hyperrectangle $\Theta \in \mathbb{R}^{n_\theta}$, i.e.

$$\theta_i(t) \in [\underline{\theta}_i, \overline{\theta}_i],\ i = 1, \ldots, n_\theta, \tag{2}$$

with symbol $'$ denoting the matrix transpose. The vertex set of Θ is denoted by Θ_v. Similarly, the rate of variation of the scheduling parameter vector $\dot{\boldsymbol{\theta}}(t)$ belongs to a hyperrectangle $\Delta \in \mathbb{R}^{n_\theta}$, i.e.

$$\dot{\theta}_i(t) \in [\underline{\delta}_i, \overline{\delta}_i],\ i = 1, \ldots, n_\theta, \tag{3}$$

and Δ_v denotes the set of vertices of Δ.

The plant model is assumed to be strictly proper, which is the characteristic of all physical systems. Moreover, proper models can easily be converted to strictly proper models by considering a high bandwidth filter for the output sensors.

It is assumed that the plant matrices depend affinely on the scheduling parameter. This means that the system matrix $A_g(\boldsymbol{\theta}(t))$ can be represented as

$$A_g(\boldsymbol{\theta}(t)) = A_{g_0} + \sum_{i=1}^{n_\theta} \theta_i(t) A_{g_i}, \tag{4}$$

and similarly the input matrix $B_g(\boldsymbol{\theta}(t))$. In order to keep the closed-loop matrices affine in $\boldsymbol{\theta}(t)$ and simplify the presentation of results, the scheduling parameter vector appears only in one of the vectors B_g or C_g. The results are presented for the case that B_g is a function of the scheduling parameters, but similar results can be developed for the other case, straightforwardly.

2.2 Controller structure

The goal of presented method is design of a fixed-order LPV dynamic output-feedback controller $K(\boldsymbol{\theta}(t))$ that stabilizes the given plant (1) in the presence of limited scheduling parameter variations. The structure of the LPV controller $K(\boldsymbol{\theta}(t))$ is assumed as

$$\begin{aligned}\dot{\mathbf{x}}_k(t) &= A_k(\boldsymbol{\theta}(t))\mathbf{x}_k(t) + B_k(\boldsymbol{\theta}(t))(\mathbf{r}(t) - \mathbf{y}(t)) \\ \mathbf{u}(t) &= C_k\mathbf{x}_k(t) + D_k(\mathbf{r}(t) - \mathbf{y}(t)),\end{aligned} \tag{5}$$

where $\mathbf{x}_k(t)$ represents the vector of controller states, and $\mathbf{r}(t)$ is the vector of reference signals.

Dependence of the controller matrices on the scheduling parameter $\boldsymbol{\theta}(t)$ is assumed affine, for example

$$A_k(\boldsymbol{\theta}(t)) = A_{k_0} + \sum_{i=1}^{n_\theta} \theta_i(t) A_{k_i}. \tag{6}$$

and similarly for $B_k(\boldsymbol{\theta}(t))$. In the rest of this paper dependence of $\boldsymbol{\theta}$, $\dot{\boldsymbol{\theta}}$ and other signals on time is implied.

By combining the plant and controller structure the following closed-loop system representation is obtained:

$$\begin{aligned}\begin{bmatrix}\dot{\mathbf{x}}_g \\ \dot{\mathbf{x}}_k\end{bmatrix} &= \begin{bmatrix} A_g(\boldsymbol{\theta}) - B_g(\boldsymbol{\theta})D_kC_g & B_g(\boldsymbol{\theta})C_k \\ -B_k(\boldsymbol{\theta})C_g & A_k(\boldsymbol{\theta})\end{bmatrix}\begin{bmatrix}\mathbf{x}_g \\ \mathbf{x}_k\end{bmatrix} \\ &+ \begin{bmatrix} B_g(\boldsymbol{\theta})D_k \\ B_k(\boldsymbol{\theta})\end{bmatrix}\mathbf{r} \\ \mathbf{y} &= [C_g\ 0]\begin{bmatrix}\mathbf{x}_g \\ \mathbf{x}_k\end{bmatrix}.\end{aligned} \tag{7}$$

To shorten the presentation, the closed-loop matrices are denoted by $A_{cl}(\boldsymbol{\theta})$, $B_{cl}(\boldsymbol{\theta})$ and C_{cl}, and the closed-loop state vector by $\mathbf{x} = [\mathbf{x}_g'\ \mathbf{x}_k']'$.

2.3 Stability conditions

To examine the stability of the closed-loop LPV system, a Lyapunov function quadratic in state and affine in the scheduling parameter can be used:

$$V(\mathbf{x}) = \mathbf{x}'P(\boldsymbol{\theta})\mathbf{x}, P(\boldsymbol{\theta}) = P_0 + \sum_{i=1}^{n_\theta} \theta_i P_i. \tag{8}$$

The first well-known condition for the stability is $P(\boldsymbol{\theta}) > 0$ for $\forall \boldsymbol{\theta} \in \Theta$. The second one is that the derivative of $V(\mathbf{x})$ is negative at any time instant. Deriving the Lyapunov function (8) and combining it with dynamics of an unforced system $\dot{\mathbf{x}} = A_{cl}(\boldsymbol{\theta})\mathbf{x}$ leads to expression

$$\dot{V}(\mathbf{x}) = \mathbf{x}'[A_{cl}'(\boldsymbol{\theta})P(\boldsymbol{\theta}) + P(\boldsymbol{\theta})A_{cl}(\boldsymbol{\theta}) + P(\dot{\boldsymbol{\theta}}) - P_0]\mathbf{x}. \tag{9}$$

So, the closed-loop stability condition for an LPV system can be written as

$$\begin{aligned}A_{cl}'(\boldsymbol{\theta})P(\boldsymbol{\theta}) + P(\boldsymbol{\theta})A_{cl}(\boldsymbol{\theta}) + P(\dot{\boldsymbol{\theta}}) - P_0 < 0 \\ P(\boldsymbol{\theta}) > 0,\ \forall(\boldsymbol{\theta}, \dot{\boldsymbol{\theta}}) \in \Theta \times \Delta.\end{aligned} \tag{10}$$

The left hand side of the inequality is polynomial in $(\boldsymbol{\theta}, \dot{\boldsymbol{\theta}})$. This means that in general the infinite number of inequalities in (10) cannot be straightforwardly replaced by a finite inequality set without loosing either the full guarantee of stability or introducing some conservatism. On the other hand, the controller parameters in $A_{cl}(\boldsymbol{\theta})$ are multiplied by Lyapunov matrix parameters $P(\boldsymbol{\theta})$ which makes the above inequality bilinear.

3. FIXED-ORDER LPV CONTROLLER DESIGN

The main idea in this approach is to present an inner convex approximation of the stability condition (10) by decoupling $A_{cl}(\boldsymbol{\theta})$ from $P(\boldsymbol{\theta})$. This is performed by introducing slack matrices. First, some definitions and lemmas useful for the representation of the convex set of fixed-order LPV controllers are presented.

The KYP lemma for continuous-time systems states that the transfer function $H(s) = C(sI - A)^{-1}B + D$ is Strictly Positive Real (SPR) transfer function if and only if there exists a matrix $P = P' > 0$ such that

$$\begin{bmatrix} A'P + PA & PB - C' \\ B'P - C & -D - D' \end{bmatrix} < 0. \tag{11}$$

By the Schur complement lemma Boyd et al. (1994), the SPRness of the system implies its stability in Lyapunov sense. Two slack matrices are introduced to enable using the KYP lemma for the controller design. Slack matrix M should enable decoupling of matrices A and P in the KYP lemma. The second slack matrix is the similarity transformation matrix T. Namely, observe the transfer function $H(s) = (T^{-1}AT - M)(sI - T^{-1}AT)^{-1}I + I$. For this transfer function the KYP lemma takes the following form:

$$\begin{bmatrix} T'A'(T')^{-1}P + PT^{-1}AT & P - T'A'(T')^{-1} + M' \\ P - T^{-1}AT + M & -2I \end{bmatrix} < 0. \tag{12}$$

Comparing to the method presented in Z. Emedi and A. Karimi (2013), the matrix T is introduced here to provide the additional degree of freedom in the controller design. For a stable LTI system with state matrix A and appropriate Lyapunov matrix P, a matrix M such that (12) is satisfied exists even if $T = I$. But, the same cannot be concluded if matrix A belongs to a polytope, so matrix T relaxes the problem of finding an appropriate M.

As the state matrix A is coupled with Lyapunov matrix P in (12), this inequality is not suitable for the controller design using the convex optimisation tools. To overcome this, an equivalent matrix inequality is introduced.

Lemma 1 The following matrix inequality is equivalent to (12):

$$\begin{bmatrix} M_T'A + A'M_T & P_T + A'X + M_T' \\ P_T + M_T + XA & -2X \end{bmatrix} < 0, \tag{13}$$

where $M_T = (T')^{-1}MT^{-1}$, $P_T = (T')^{-1}PT^{-1}$ and $X = (T')^{-1}T^{-1}$.

Proof. Pre-multiplication of (13) by

$$\begin{bmatrix} T' & -M'T' - PT' \\ 0 & T' \end{bmatrix}$$

and post-multiplication by its transpose leads to (12). As pre- and post-multiplication by the non-singular matrix and its inverse does not change negative definiteness of the matrix, equivalence is ensured. □

In (13) matrices A and P are decoupled. Based on equivalent inequalities (12) and (13), the following characterisation of the set of stabilizing LPV controllers for (1) is proposed.

Theorem 1 Suppose that the LPV plant model is described by (1) and (4) and that the scheduling parameter and its variation rate belong to $[\underline{\theta}, \overline{\theta}]$ and $[\underline{\delta}, \overline{\delta}]$. Then, given matrices M_T and X, the controller in (5) and (6) stabilizes the LPV model for any allowable scheduling parameter trajectory if

$$\begin{bmatrix} -A_{cl}'(\boldsymbol{\theta})M_T - M_T'A_{cl}(\boldsymbol{\theta}) + P_T(\boldsymbol{\theta}) - P_{0_T} & (*) \\ P_T(\boldsymbol{\theta}) + XA_{cl}(\boldsymbol{\theta}) + M_T & -2X \end{bmatrix} < 0, \tag{14}$$

$$P_T(\boldsymbol{\theta}) > 0 \quad , \quad \forall \boldsymbol{\theta} \in \Theta_v, \forall \dot{\boldsymbol{\theta}} \in \Delta_v.$$

Symbol $(*)$ substitutes terms which ensure the symmetry of the matrix.

Proof. Observe that the left-hand side of (14) can be represented as a symmetric matrix expression affine in vector $\phi' = [\boldsymbol{\theta}' \, \dot{\boldsymbol{\theta}}']$. As $\phi \in \Phi = \Theta \times \Delta$, it follows that matrix inequality (14) is satisfied for all $\boldsymbol{\theta} \in \Theta$ and $\dot{\boldsymbol{\theta}} \in \Delta$. Next, let the relations $M = T'M_TT$ and $P(\boldsymbol{\theta}) = T'P_T(\boldsymbol{\theta})T$ be introduced, where T is a non-singular matrix satisfying $X = (T')^{-1}T^{-1}$. Pre-multiplication of (14) by the matrix

$$\begin{bmatrix} T' & -M'T' - P(\boldsymbol{\theta})T' \\ 0 & T' \end{bmatrix}$$

and post-multiplication by its transpose leads to

$$\begin{bmatrix} T'A_{cl}(\boldsymbol{\theta})'(T')^{-1}P(\boldsymbol{\theta}) + (*) + P(\dot{\boldsymbol{\theta}}) - P(0) & (*) \\ P(\boldsymbol{\theta}) + M - T^{-1}A_{cl}(\boldsymbol{\theta})T & -2I \end{bmatrix} < 0.$$

But, application of the Schur complement lemma directly implies validity of the stability condition (10) (for $T^{-1}A_{cl}(\boldsymbol{\theta})T$ by $P(\boldsymbol{\theta})$, hence for $A_{cl}(\boldsymbol{\theta})$ by $P_T(\boldsymbol{\theta})$). So, the system is stabilized for bounded scheduling parameter variations. □

Values of matrices M_T and X need to be known in order to apply this theorem for the fixed-order LPV controller design. Assume that an initial controller is available for the LTI system that corresponds to the center of the polytope Θ. This controller may be computed using some standard fixed-order controller design approach. Then this controller is used instead of the LPV controller in (14), and (14) is treated as the convex programming problem with variables M_T, X and P_T. Using so obtained values of M_T and X in (14) now leads to the convex programming problem in variables A_k, B_k, C_k, D_k and P_T, so in the second step fixed-order LPV controller is synthesized.

4. EXPERIMENTAL RESULTS

In this section, the application of the proposed method to the 2DOF gyroscope experimental setup is described. The focus is on the LPV modeling of the experimental setup, initial LTI controller and desired LPV controller design, and experimental results obtained from the application of LPV controller on the setup.

4.1 Experimental setup description

The gyroscope experimental setup used for performing control experiments described in this paper is shown on

Fig. 1. Quanser gyroscope experimental platform (Quanser Consulting Inc. (Rev. 1.0)).

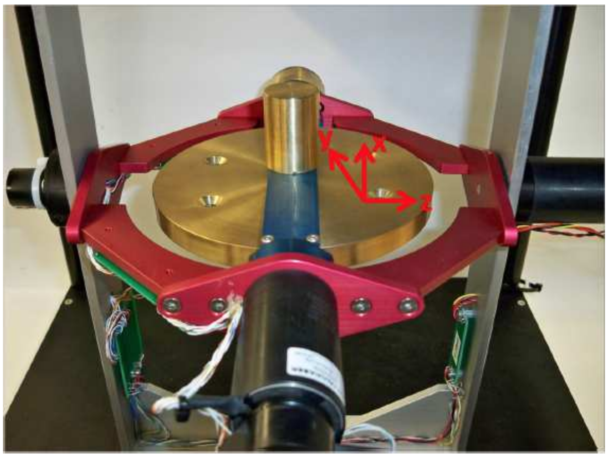

Fig. 2. Axis of the rotating coordinate frame (Quanser Consulting Inc. (Rev. 1.0)).

Figure 1. Figure 2 illustrates the reference frame xyz that rotates together with the brass disc and the blue frame. The brass disc rotates around the axis x passing through its center and perpendicular to the disc. Axis y represents the axis around which blue frame rotates together with brass disc. Red frame rotates around the axis Z of the inertial reference frame (not to be confused with axis z). In the experiment described in this paper grey frame is fixed.

The angular positions of the disc, blue and red frame are measured using quadrature encoders. Three DC motors are used to actuate the disc, the blue and the red frame about the axis x, y and Z, respectively. Data acquisition is performed using the National Instruments DAQ card and Mac Pro computer. A power amplifier is used to convert the voltage output of the DAQ card to current signals applied to the DC motors. A specific LabView virtual instrument is designed for real-time communication and control. Its role is to acquire all the measurements from the DAQ card and condition them properly, to serve as a user interface, and to calculate control signals and store all the relevant data from the experiment.

4.2 Experimental setup modeling

The nonlinear model of the 2DOF gyroscope is provided. LPV model is built based on it using some approximations.

Nonlinear model and approximation First-principle modeling of the 2DOF gyroscope is explained in details in Cannon (2003). The model takes the following form:

$$\begin{aligned} J_y\ddot{\phi} - J_x^d\dot{\upsilon}\dot{\psi}\cos\phi + (J_z - J_x)\dot{\psi}^2\sin\phi\cos\phi = M_b \\ (J_Z^r + J_z\cos^2\phi + J_x\sin^2\phi)\ddot{\psi} + J_x^d\dot{\upsilon}\dot{\phi}\cos\phi + \\ +2(J_x - J_z)\dot{\psi}\dot{\phi}\sin\phi\cos\phi = M_r. \end{aligned} \tag{15}$$

Dependence of all the signals on time is implied.

Angle υ denotes the angular position of the disc around its axis of rotation x. Similarly, angle ϕ represents the angular position of the blue frame about y, and ψ the angular position of the red frame about Z. For the convenience, another axis of rotation named z is introduced. Axis z represents the third axis (aside from x and y) of the Cartesian system that rotates together with the disc and the blue frame. J_x, J_y and J_z are the total moments of inertia of disc and blue frame around the axis x, y and z, respectively. J_Z^r is the moment of inertia of the red frame around the axis Z, and J_x^d that of the disc around the axis x. Total external torque around the axis of rotation of the blue gimbal is denoted by M_b, and M_r is the total external torque around the axis of rotation of the red gimbal. As the static friction can be considered negligible, M_b and M_c represent the torques produced by appropriate motors.

The modeling goal is to build an LPV model scheduled by parameter $\theta = \dot{\upsilon}$ around the set point (ϕ_0, ψ_0). For this purpose the approximation of the nonlinear model (15) is performed. Assume that the first-order Taylor approximation of (15) is obtained, with $\phi = \phi_0 + \Delta\phi$ and $\psi = \psi_0 + \Delta\psi$. Taking into account $\dot{\phi}_0 = \ddot{\phi}_0 = 0$ and $\dot{\psi}_0 = \ddot{\psi}_0 = 0$, as well as $\sin\Delta\phi \approx \Delta\phi$ and $\cos\Delta\phi \approx 1$, the following linearized model is obtained:

$$\begin{aligned} J_y(\ddot{\Delta\phi}) - J_x^d\dot{\upsilon}(\dot{\Delta\psi})\cos\phi_0 + \\ (J_z - J_x)(\dot{\Delta\psi})^2\sin\phi_0\cos\phi_0 = M_b \\ (J_Z^r + J_z\cos^2\phi_0)\ddot{\Delta\psi} + J_x^d\dot{\upsilon}\dot{\Delta\phi}\cos\phi_0 + \\ +2(J_x - J_z)\dot{\Delta\psi}\dot{\Delta\phi}\sin\phi_0\cos\phi_0 = M_r \end{aligned} \tag{16}$$

The manual Quanser Consulting Inc. (Rev. 1.0) states that $J_x = 0.0074kgm^2$ and $J_z = 0.0056kgm^2$. Further, it is reasonable to assume that in the experiment $\left|\dot{\Delta\psi}\right|$ is of order of $1\frac{rad}{s}$. On the other hand, $J_x^d = 0.0056kgm^2$, and the value of the angular speed $\dot{\upsilon}$ at which disc rotates in the experiment is of order $150\frac{rad}{s}$. With all these values in mind, and the fact that $|\sin\phi_0| \leq 1$, it is reasonable to conclude that

$$\left|J_x^d \dot{\upsilon}(\dot{\Delta\phi})\cos\phi_0\right| \gg \left|2(J_x - J_z)(\dot{\Delta\psi})(\dot{\Delta\phi})\sin\phi_0\cos\phi_0\right|. \tag{17}$$

This leads to the following simplified gyroscope model around the set point (ϕ_0, ψ_0):

$$\begin{aligned} J_y\ddot{\Delta\phi} - J_x^d\dot{\upsilon}\dot{\Delta\psi}\cos\phi_0 &= M_b \\ (J_Z^r + J_z\cos^2\phi_0)\ddot{\Delta\psi} + J_x^d\dot{\upsilon}\dot{\Delta\phi}\cos\phi_0 &= M_r\ . \end{aligned} \tag{18}$$

LPV model The set point chosen for the experiment is $(\phi_0, \psi_0) = (0, 0)$. Consequently, $\Delta\psi$ and $\Delta\phi$ in (18) can be replaced by ψ and ϕ, respectively. Denoting $J_Z^0 = J_Z^r + J_z\cos^2\phi_0 = J_Z^r + J_z$, with numerical value $J_Z^0 = 0.0342kgm^2$, leads to the following LPV model scheduled in $\dot{\upsilon}$:

$$\begin{aligned} J_y\ddot{\phi} - J_x^d\dot{\upsilon}\dot{\psi} &= M_b \\ J_Z^0\ddot{\psi} + J_x^d\dot{\upsilon}\dot{\phi} &= M_r\ , \end{aligned} \tag{19}$$

where $J_y = 0.0026kgm^2$.

Next, the torques M_b and M_c can be approximated by $M_b = K_b u_b$ and $M_r = K_r u_r$, ignoring dynamics of the power amplifier and motors. Here, u_b and u_r are the control inputs in volts, sent through the DAQ card to the power amplifier. Based on the manual values, it can be concluded that $K_b = K_r = 0.03985\frac{Nm}{V}$.

Finally, the following LPV model in form (1) is obtained:

$$\dot{\mathbf{x}}_g(t) = \begin{bmatrix} 0 & 1 & 0 & 0 \\ 0 & 0 & 0 & \frac{J_x^d}{J_y}\theta \\ 0 & 0 & 0 & 1 \\ 0 & -\frac{J_x^d}{J_Z^0}\theta & 0 & 0 \end{bmatrix} \mathbf{x}_g(t) + \begin{bmatrix} 0 & 0 \\ \frac{K_b}{J_y} & 0 \\ 0 & 0 \\ 0 & \frac{K_r}{J_Z^0} \end{bmatrix} \mathbf{u}(t) \tag{20}$$

$$\mathbf{y}(t) = \begin{bmatrix} 1 & 0 & 0 & 0 \\ 0 & 0 & 1 & 0 \end{bmatrix} \mathbf{x}_g(t),$$

with $\mathbf{x}_g(t) = [\phi(t)\ \dot{\phi}(t)\ \psi(t)\ \dot{\psi}(t)]'$, $u(t) = [u_b(t)\ u_r(t)]'$ and $\theta = \dot{\upsilon}$.

4.3 Control System Design

As described in Section 3, first the initial LTI controller has to be designed. Next, based on this LTI controller, LPV controller for a range of scheduling parameters is designed. Details are provided below.

Initial LTI controller design. The goal of the controller design is to ensure good tracking of the angular positions of the blue and red frames to given step references. As the first step, a second-order LTI controller is designed for the nominal value of the scheduling parameter $\theta = 150\frac{rad}{s}$. Function `hinfstruct` of the Matlab® Robust Control Toolbox™ is used for the fixed-order LTI controller design. The plant model (20) for the fixed value of scheduling parameter $\theta = 150\frac{rad}{s}$ is adapted into the classical LFT form for the use with `hinfstruct`. Position references $r_b(t)$ and $r_r(t)$ are chosen as external inputs, control signals $u_b(t)$ and $u_r(t)$ as internal inputs, and position error signals $e_b(t) = r_b(t) - x_{g_1}$ and $e_r(t) = r_r(t) - x_{g_3}$ as measured outputs.

The first goal of a nominal LTI controller design is to obtain good tracking performance. For this reason the error signals $e_b(t)$ and $e_r(t)$ are chosen as the performance outputs. To obtain good tracking for step reference, these two performance outputs are weighted by performance filter

$$W_1 = \begin{bmatrix} \frac{1}{s + 10^{-5}} & 0 \\ 0 & \frac{1}{s + 10^{-5}} \end{bmatrix}.$$

On the other hand, to ensure that the given controller can be applied on the real system, magnitude of the control inputs has to be kept below the saturation levels. To ensure this, two performance outputs corresponding to control inputs $u_b(t)$ and $u_r(t)$ are weighted by

$$W_3 = \begin{bmatrix} 0.15 & 0 \\ 0 & 0.15 \end{bmatrix}.$$

Such a specification leads to the following optimal second-order LTI controller:

$$\left[\begin{array}{c|c} A_k & B_k \\ \hline C_k & D_k \end{array}\right] = \left[\begin{array}{cc|cc} -0.4029 & -94.43 & 37.3 & 39.1 \\ 65.54 & -133.8 & 49.65 & 19.38 \\ \hline -5.392 & -24.21 & 9.683 & 1.15 \\ -23.18 & 17.85 & 5.834 & 5.138 \end{array}\right]. \tag{21}$$

LPV controller design. For the given experiment, the bounds on the scheduling parameter and its derivative are chosen as $\Theta = [125\frac{rad}{s}, 175\frac{rad}{s}]$ and $\Delta = [-10\frac{rad}{s^2}, 10\frac{rad}{s^2}]$. The algorithm for the fixed-order LPV controller design is initialized using the LTI controller presented in the previous subsection. This leads to the LPV controller $A_k(\theta), B_k(\theta), C_k(\theta), D_k(\theta))$ given by

$$A_k(\theta) = \begin{bmatrix} -15.9183 + 0.1550\theta & -61.9083 - 0.3490\theta \\ 40.8114 + 0.2349\theta & -85.0970 - 0.4977\theta \end{bmatrix}$$

$$B_k(\theta) = \begin{bmatrix} 26.3020 + 0.1483\theta & 39.8019 - 0.0009\theta \\ 35.6540 + 0.1785\theta & 14.8075 + 0.0301\theta \end{bmatrix}$$

$$C_k(\theta) = \begin{bmatrix} -5.8025 + 0.0136\theta & -15.9180 - 0.1083\theta \\ -19.1979 - 0.0365\theta & 6.1528 + 0.0927\theta \end{bmatrix}$$

$$D_k(\theta) = \begin{bmatrix} 8.6381 + 0.0305\theta & 4.4201 - 0.0249\theta \\ 8.8580 - 0.0249\theta & 9.7777 - 0.0243\theta \end{bmatrix}$$

As the given LPV controller has to be applied on the system using a digital computer, a discretisation has to be performed. The following approximations, based on the first-order Taylor series, are used:

$$A_k^d(\theta) = e^{A_k(\theta)} \approx I + T_s A_k(\theta) = (I + T_s A_{k_0}) + \theta T_s A_{k_1}$$

$$B_k^d(\theta) = A_k^{-1}(\theta)(A_k^d(\theta) - I)B_k(\theta) \approx T_s B_k(\theta).$$

Sampling time is chosen as $T_s = 1ms$. This leads to a discretized LPV controller with preserved linear dependence on the scheduling parameter θ.

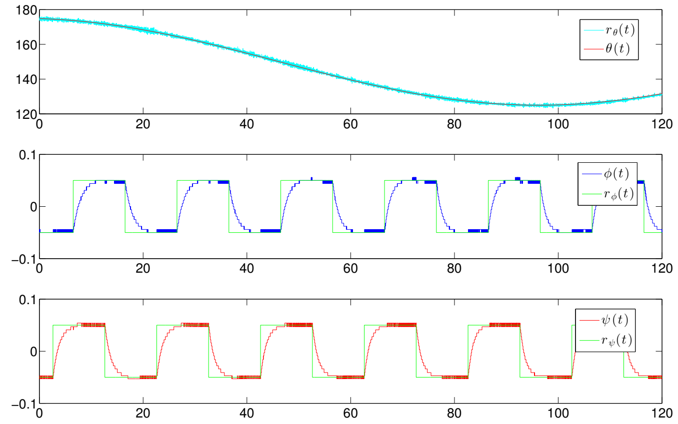

Fig. 3. Disc speed, blue frame and red frame position evolution during the experiment.

4.4 Experimental results

The goal of experiment is to illustrate that designed LPV controller preserves good performance in the presence of scheduling parameter variations. To test this assumption, the following experiment is performed. Value of the angular velocity of the disc $\dot{\upsilon}$, i.e. scheduling parameter θ, is made to track sinusoidal reference between $125\frac{rad}{s}$ and $175\frac{rad}{s}$. Simple first-order transfer function fitting provides the model between the voltage sent through the DAQ card and angular speed of disc:

$$G_{sl}(s) = \frac{6.052}{s + 0.0025}.$$

Movement of blue and red frames does not have a strong influence on the rotational speed of the disc. Hence, a simple proportional controller $K_{sl} = 0.3305$ is used to ensure this tracking, successfully as it can be observed on the first graph of Figure 3.

References for positions of the blue and red frame are given as rectangular functions with period of $10s$. Figure 3 illustrates comparison between the obtained response and the reference for the blue and the red frame. Tracking performance is excellent for both frames.

5. CONCLUSIONS

In this paper, design of fixed-order LPV controller and its application to a 2DOF gyroscope experimental setup are considered. LPV model of the system is obtained by approximating the nonlinear model of the system. Then, a second-order continuous-time LPV MIMO controller is designed, discretized and applied in the real-time experiment. Experimental results illustrate good tracking performance of the control system in the presence of variations of the disc angular velocity as a scheduling parameter.

REFERENCES

Apkarian, P. and Adams, R.J. (1998). Advanced gain-scheduling techniques for uncertain systems. *IEEE Transactions on Control Systems Technology*, 6(1), 21–32.

Apkarian, P. and Gahinet, P. (1995). A convex characterization of gain-scheduled H_∞ controllers. *IEEE Transactions on Automatic Control*, 40(5), 853–864.

Balas, G.J. (2002). Linear, parameter-varying control and its application to a turbofan engine. *International Journal of Robust and Nonlinear Control*, 12(9), 763–796.

Boyd, S., Ghaoui, L.E., Feron, E., and Balakrishnan, V. (1994). *Linear Matrix Inequalities in System and Control Theory*. SIAM, Philadelphia.

Cannon, R.H. (2003). *Dynamics of physical systems*. Courier Dover Publications.

F. D. Adegas, C. Sloth, and J. Stoustrup (2012). Structured linear parameter varying control of wind turbines. In *Control of Linear Parameter Varying Systems with Applications*, 303–337. Springer.

F. D. Bianchi, R. J. Mantz, and C. F. Christiansen (2004). Control of variable-speed wind turbines by LPV gain scheduling. *Wind Energy*, 7, 1–8.

F. Wu, A. Packard, and G. Balas (1995). LPV control design for pitch-axis missile autopilots. In *34th IEEE Conference on Decision and Control*, volume 1, 188–193. IEEE.

F. Wu, X. H. Yang, A. Packard, and G. Becker (1996). Induced l_2-norm control for LPV system with bounded parameter variation rate. In *Proceedings of the American Control Conference*. Seattle, Washington, USA.

G. Panzani, S. Formentin, and S. M. Savaresi (2012). Active motorcycle braking via direct data-driven load transfer scheduling. In *16th IFAC Symposium on System Identification, SYSID 2012*. Brussels, Belgium.

Geromel, J.C., Korogui, R.H., and Bernussou, J. (2007). H_2 and H_∞ robust output feedback control for continuous time polytopic systems. *IET Control Theory and Applications*, 1(5), 1541–1549.

H. Khatibi and A. Karimi (2010). H_∞ controller design using an alternative to Youla parameterization. *IEEE Transactions on Automatic Control*, 55(9), 2119–2123.

Henrion, D., Sebek, M., and Kucera, V. (2003). Positive polynomials and robust stabilization with fixed-order controllers. *IEEE Transactions on Automatic Control*, 48(7), 1178–1186.

J. C. Geromel, M. C. de Oliveira, and L. Hsu (1998). Lmi characterization of structural and robust stability. *Linear Algebra and its Applications*, 285, 69–80.

J-M Biannic and P. Apkarian (1999). Missile autopilot design via a modified LPV synthesis technique. *Aerospace Science and Technology*, 3(3), 153–160.

L. H. Crater and J. S. Shamma (1996). Gain-scheduled bank-to-turn autopilot design using linear parameter varying transformations. *Journal of guidance, control, and dynamics*, 19(5), 1056–1063.

Leith, D.J. and Leithead, W.E. (2000). Survey of gain-scheduling analysis and design. *International Journal of Control*, 73(11), 1001–1025.

P. C. Pellanda, P. Apkarian, and H. D. Tuan (2002). Missile autopilot design via a multi-channel LFT/LPV control method. *International Journal of Robust and Nonlinear Control*, 12(1), 1–20.

Quanser Consulting Inc. (Rev. 1.0). *Gyroscope Position Control*. 119 Spy Court, Markham, Ontario, L3R 5H6,

Canada. URL http://www.quanser.com.
S. Formentin, D. Piga, R. Tóth, and S. Savaresi (2013). Direct data-driven control of linear parameter-varying systems. In *52nd IEEE Conference on Decision and Control*. Florence, Italy.
Sato, M. (2011). Gain-scheduled output-feedback controllers depending solely on scheduling parameters via parameter-dependent Lyapunov functions. *Automatica*, 47, 2786–2790.
Shamma, J. and Athans, M. (1991). Guaranteed properties of gain scheduled control for linear parameter-varying plants. *Automatica*, 27(3), 559–564.
Shamma, J.S. (2012). An overview of LPV systems. In *Control of Linear Parameter Varying Systems with Applications*, 3–26. Springer.
W. Gilbert, D. Henrion, J. Bernussou, and D. Boyer (2010). Polynomial LPV synthesis applied to turbofan engines. *Control Engineering Practice*, 18, 1077–1083.
Wassink, M.G., van de Wal, M., Scherer, C., and Bosgra, O. (2005). LPV control for a wafer stage: beyond the theoretical solution. *Control Engineering Practice*, 13, 231–245.
Z. Emedi and A. Karimi (2012). Fixed-order LPV controller design for rejection of a sinusoidal disturbance with time-varying frequency. In *IEEE Multi-Conference on Systems and Control*. Dubrovnik, Croatia.
Z. Emedi and A. Karimi (2013). Fixed-order LPV controller design for LPV systems by convex optimization. In *5th IFAC Symposium on System Structure and Control*. Grenoble, France.